Response of vegetation distribution, ecosystem productivity, and fire to climate change scenarios for California

**James M. Lenihan · Dominique Bachelet ·
Ronald P. Neilson · Raymond Drapek**

Abstract The response of vegetation distribution, carbon, and fire to three scenarios of future climate change was simulated for California using the MC1 Dynamic General Vegetation Model. Under all three scenarios, Alpine/Subalpine Forest cover declined, and increases in the productivity of evergreen hardwoods led to the displacement of Evergreen Conifer Forest by Mixed Evergreen Forest. Grassland expanded, largely at the expense of Woodland and Shrubland, even under the cooler and less dry climate scenario where increased woody plant production was offset by increased wildfire. Increases in net primary productivity under the cooler and less dry scenario contributed to a simulated carbon sink of about 321 teragrams for California by the end of the century. Declines in net primary productivity under the two warmer and drier scenarios contributed to a net loss of carbon ranging from about 76 to 129 teragrams. Total annual area burned in California increased under all three scenarios, ranging from 9–15% above the historical norm by the end of the century. Annual biomass consumption by fire by the end of the century was about 18% greater than the historical norm under the more productive cooler and less dry scenario. Under the warmer and drier scenarios, simulated biomass consumption was initially greater, but then at, or below, the historical norm by the end of the century.

1 Introduction

California is one of the most climatically and biologically diverse areas in the world. There is more diversity in the state's land forms, climate, ecosystems, and species than in any

J. M. Lenihan · R. P. Neilson · R. Drapek
USDA Forest Service Pacific Northwest Research Station, Corvallis, OR 97731, USA

D. Bachelet
Oregon State University, Corvallis, OR 97331, USA

J. M. Lenihan (✉)
USFS Pacific Northwest Research Laboratory, 3200 SW Jefferson Way, Corvallis, OR, USA
e-mail: lenihan@fsl.orst.edu

🖄 Springer

comparably sized region in the USA (Holland and Keil 1995). This diversity of habitats sustains a greater level of species diversity and endemism than is found in any other region of the nation (Davis et al. 1998). Much of California's biological wealth is threatened by the state's burgeoning population and the consequent impacts on the landscape. Throughout the state, natural habitats have been and continue to be altered and fragmented, endangering the state's biological diversity (Barbour et al. 1993).

In the future, global climate change will increasingly interact with and intensify the pressures of a growing population on the natural ecosystems of California. Projections of the response of the natural systems to global climate change must incorporate the interaction of multiple factors (e.g., simultaneous changes in temperate, precipitation, and CO_2 concentration). Currently, there are very few experiments measuring the response of naturally occurring ecosystems to changes in multiple environmental factors (Dukes et al. 2005). Single-factor whole-ecosystem experiments (e.g., free-air CO2 enrichment or FACE experiments) are more numerous, but are necessarily case studies limited to specific assemblages of species and climatic zones (Norby and Luo 2004). However, more generalized analyses of the sensitivity of natural ecosystems to changes in multiple interacting factors can be made using ecosystem models that integrate information from direct experimentation.

In a previous study, the MC1 Dynamic General Vegetation Model (DGVM) generated simulations of the response of vegetation distribution, ecosystem productivity, and fire to the observed historical climate and to scenarios of potential future climate change for California (Lenihan et al. 2003). The future climate scenarios were constructed from output generated by two general circulation models (the Hadley Climate Center HADCM2 model and the National Center for Atmospheric Research (NCAR) PCM model), both run into the future using a "business as usual" emission scenario (IS92a) developed by the Intergovernmental Panel on Climate Change (IPCC; Kattenberg et al. 1996). Improved understanding of the driving forces in emissions motivated the development of a new set of IPCC emission scenarios described in the Special Report on Emission Scenarios (SRES; IPCC 2000). Hayhoe et al. (2004) described future shifts in the distribution of California vegetation types simulated by MC1 for climate scenarios incorporating two of the new SRES emission scenarios.

In 2005, the California Climate Change Center initiated the multi-disciplinary "Climate Scenarios" project to analyze potential climate change impacts on several different sectors of the state in response to Governor Schwarzenegger's Executive Order S-3-05 (Cayan et al. 2006). Future climate scenarios for the study were selected from the IPCC Fourth Climate Assessment which provides several simulations generated by the latest state-of-the-art GCMs using the new SRES emission scenarios. Four climate scenarios were chosen to represent output from GCMs of both low and medium-high climate sensitivity [e.g., the NCAR PCM model and the Geophysical Fluids Dynamic Laboratory (GFDL) CM2.1 model] and both lower and medium-high emissions scenarios (SRES-B1 and SRES-A2 respectively). Here we describe the results of MC1 simulations for three of the climate scenarios which contributed to the project's analysis of potential climate change impacts on the forest/fire sector in California.

2 Methods

2.1 The MC1 model

MC1 is a dynamic vegetation model (DGVM) that simulates plant type mixtures and vegetation types; the movement of carbon, nitrogen, and water through ecosystems; and fire disturbance.

MC1 routinely generates century-long, regional-scale simulations on relatively coarse-scale data grids (Daly et al. 2000; Bachelet et al. 2000, 2001; Aber et al. 2001; Lenihan et al. 2003). The model reads soil and monthly climate data, and calls interacting modules that simulate biogeochemistry, biogeography, and fire disturbance (Bachelet et al. 2001).

2.1.1 Biogeochemistry module

The biogeochemistry module is a modified version of the Century model (Parton et al. 1994) which simulates plant growth, organic matter decomposition, and the movement of water and nutrients through the ecosystem. Plant growth is determined by empirical functions of temperature, moisture, and nutrient availability which decrement set values of maximum potential productivity. In this study, plant growth was assumed not to be limited by nutrient availability. The effect of an increase in atmospheric carbon dioxide (CO_2) is simulated using factors that increase maximum potential productivity and reduce the moisture constraint on productivity. Grasses compete with woody plants for soil moisture in the upper soil layers where both are rooted, while the deeper-rooted woody plants have sole access to moisture in deeper layers. The growth of grass may be limited by reduced light levels in the shade cast by woody plants. The values of model parameters that control woody plant and grass growth are adjusted with shifts in the life-form mixture determined annually by the biogeography module. Grass production is allocated to live leaf and fine root carbon pools, while woody plant production is allocated to live leaf, fine branch, large wood, fine root, and coarse root pools. Dead leaves and fine roots are transferred to surface and root residue pools, while dead fine branch, large wood, and coarse root pools receive dead wood material from the live fine branch, large wood, and coarse root pools respectively.

2.1.2 Biogeography module

The biogeography module simulates changes in the mixture of different types of trees, shrubs, and grasses in each grid cell over time as a response to climate and fire. Woody plants are represented in the model as trees or shrubs, and as different life-forms distinguished by leaf characteristics. The three tree and shrub life-forms represented in the model are evergreen needleleaf, evergreen broadleaf, and deciduous broadleaf. The two types of grass life-forms represented in the model are C3 and C4 grasses distinguished by their response to temperature. The C3 grass life-form is most productive in relatively cool habitats, while C4 grasses are more tolerant of higher temperatures.

The biogeography module simulates the mixture of plant life-forms in each grid cell each year. Woody plants in the mixture are determined to be either trees or shrubs based on the current amount of woody plant biomass simulated by the biogeochemistry module (see Section 2.1.1). The relative proportion of different woody life-forms is determined at each annual time-step by locating the grid cell on a two-dimensional gradient of annual minimum temperature and growing season precipitation. Life-form dominance is arrayed along the minimum temperature gradient from increasing evergreen needleleaf dominance towards the low end of the gradient (−15°C) to increasing broadleaf evergreen dominance near the high end (18°C) of the gradient, and with increasing deciduous broadleaf dominance towards the midpoint of the temperature gradient. The relative proportion of the deciduous broadleaf life-form is also modulated along the growing season precipitation gradient, gradually being reduced to zero towards the low end (50 mm) of the gradient. The relative proportion of C3 and C4 grasses in the simulated plant mixture is determined by

estimating the potential productivity of each grass life-form as function of soil temperature during the three warmest consecutive months (Parton et al. 1994).

The simulated plant life-form mixture together with woody plant and grass biomass simulated by the biogeochemistry module are used by the biogeography module to determine the vegetation type that occurs at each grid cell each year. Of the 22 possible vegetation types predicted by the biogeography module, 12 occurred in the simulations for California. These types were aggregated into seven vegetation classes to simplify the visualization of results. The aggregation scheme and lists of typical regional examples in each vegetation class are listed in Table 1.

2.1.3 Fire disturbance module

The MC1 fire module simulates the occurrence, behavior, and effects of fire. The module simulates the behavior of a simulated fire event in terms of the potential rate of fire spread, fireline intensity, and the transition from surface to crown fire (Rothermel 1972; van Wagner 1993; Cohen and Deeming 1985). Several measurements of the fuel bed are required for simulating fire behavior, and they are estimated by the fire module using information provided by the other two MC1 modules. The current life-form mixture is used by the fire module to select factors that apportion live and dead biomass into different classes of live and dead fuels. The moisture content of the two live fuel classes (grasses and leaves/twigs of woody plants) are estimated from moisture at different depths in the soil provided by the biogeochemical module. Dead fuel moisture content is estimated from climatic inputs to MC1 using different functions for each of four dead fuel size-classes (Cohen and Deeming 1985).

Table 1 MC1 vegetation type aggregation scheme and regional examples of the vegetation classes

MC1 vegetation class	MC1 vegetation type	Regional examples
Alpine/Subalpine Forest	Tundra	Alpine Meadows
	Boreal forest	Lodgepole Pine Forest
		Whitebark Pine Forest
Evergreen Conifer Forest	Maritime temperate conifer forest	Coastal Redwood Forest
	Continental temperate coniferous forest	Coastal Closed-Cone Pine Forest
		Mixed Conifer Forest
		Ponderosa Pine Forest
Mixed Evergreen Forest	Warm temperate/subtropical mixed forest	Douglas Fir–Tanoak Forest
		Tanoak–Madrone–Oak Forest
		Ponderosa Pine–Blackoak Forest
Mixed Evergreen Woodland	Temperate mixed xeromorphic woodland	Blue Oak Woodland
	Temperate conifer xeromorphic woodland	Canyon Live Oak Woodland
		Northern Juniper Woodland
Grassland	C3 Grassland	Valley Grassland
	C4 Grassland	Southern Coastal Grassland
		Desert Grassland
Shrubland	Mediterranean shrubland	Chamise Chaparral
	Temperate arid shrubland	Southern Coastal Scrub
		Sagebrush Steppe
Desert	Subtropical arid shrubland	Creosote Brush Scrub
		Saltbrush Scrub
		Joshua Tree Woodland

Fire events are triggered in the model when the moisture content of the largest dead fuel class and the simulated rate of fire spread meet set thresholds. Sources of ignition (e.g., lightning or anthropogenic) are assumed to be always available. The fire occurrence thresholds were calibrated to limit the occurrence of simulated fires to only the most extreme events. Large and severe fires account for a very large fraction of the annual area burned historically (Strauss et al. 1989), and these events are also likely to be least constrained by heterogeneities in topography and fuels that are poorly represented by relatively coarse-scale modeling grids (Turner and Romme 1994). Area burned is not simulated explicitly as fire spread within a given cell, or from one cell to another. Instead, the fraction of a cell burned by a fire event is estimated as a linear function of the time since the last fire event with an adjustment made for the potential rate of fire spread. The MC1 fire module generates a trend in total area burned over the historical period that is within the limits of an independently estimated range of variability for the pre-settlement fire regime in California (Lenihan et al. 2003). Fire suppression was not simulated in this study.

The fire module simulates the consumption and mortality of dead and live vegetation carbon, which is removed from (or transferred to) the appropriate carbon pools in the biogeochemistry module. Live carbon mortality and consumption are simulated as a function of fireline intensity and the tree canopy structure (Peterson and Ryan 1986), and dead biomass consumption is simulated using functions of fuel moisture that are fuel-class specific (Anderson et al. 2005).

2.2 Climate data

The climate data used as input to the model in this study consisted of monthly time series for all the necessary variables (i.e., precipitation, minimum and maximum temperature, and vapor pressure) distributed on a 100 km^2 resolution data grid for the state of California. Spatially distributed monthly time-series data for historical (1895–2003) precipitation, temperature, and vapor pressure already existed at a 100 km^2 resolution. This dataset was developed from a subset of climate data generated by the VEMAP model (Kittel et al. 2004) and from observed California station data interpolated to the data grid by the PRISM model (Daly et al. 1994).

To construct spatially distributed climate time-series datasets for the potential future climatic periods (2004–2100) of our simulations, we used coarse-scale monthly output generated by the two general circulation models (GCMs) – the GFDL CM2.1 model and the NCAR PCM model. The GFDL model has a medium climate sensitivity of approximately 3°F for a doubling of CO_2 above pre-industrial levels, while the PCM model has a relatively low sensitivity of about 1.8°C. Both GCM models were run from the 1800s to 1995 using observed increases in greenhouse gas concentrations, and into the future using two different SRES emission scenarios. The A2 medium–high emissions scenario corresponds to a CO_2 concentration by the end of the century more than three times the pre-industrial level, while the B1 low emissions scenario results in a doubling of pre-industrial CO_2.

Sufficient climatic inputs for MC1 simulations were available from only three of the GCM-emission scenario experiments (i.e., GFDL-A2, GFDL-B1, and PCM-A2). The GFDL-A2 model run had the greatest increase in temperature (>4°C) and was the driest of the three scenarios used here. This scenario was at the high end of temperature changes over California compared to an ensemble of IPCC AR4 model simulations (Cayan et al. 2006). The GFDL-B1 and PCM-A2 runs represented moderately dry to neutral scenarios respectively, with intermediate temperature increases (<3°C) over California.

3 Results

3.1 The response of vegetation distribution to the future climate scenarios

The response of vegetation class distribution under the three future climate scenarios was determined by comparing the distribution of the most frequent vegetation type simulated for the 30-year historical period (1961–1990) against the same for the last 30 years (2071–2100) of the future scenarios (Figs. 1, 2 and 3). The overall distribution of the vegetation classes simulated for the historical period is very similar to the observed distribution of natural vegetation types in California (Lenihan et al. 2003). The simulated response of the vegetation classes in terms of changes in percentage coverage (Fig. 4) was surprisingly similar under the three future climates. There was agreement on the direction of change (i.e., decrease or increase in coverage) for all but the Desert class, and the amounts of change were comparable for several of the vegetation classes. However, these similarities in the response of class coverage were often the net result of very different responses to each scenario in terms of the spatial distribution of vegetation classes, as discussed below.

Significant declines in the extent of Alpine/Subalpine Forest were simulated under all three scenarios, especially under the warmest GFDL-A2 scenario. At high elevation sites the model responded to longer and warmer growing seasons, which favored the replacement of Alpine/Subalpine Forest by other vegetation types.
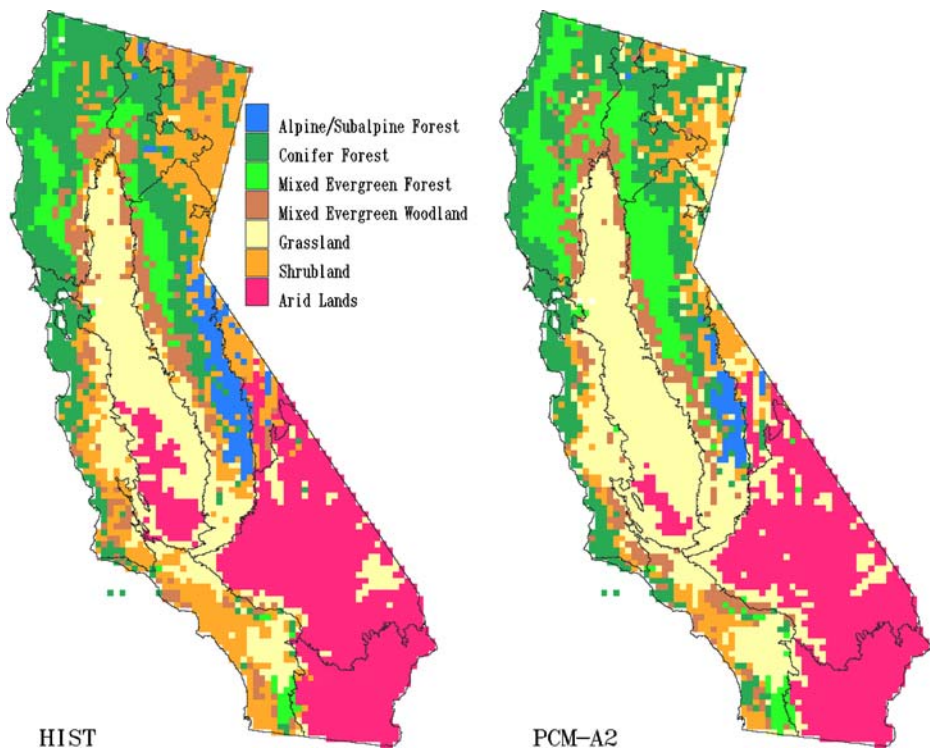

Fig. 1 Distribution of the vegetation classes simulated for the historical (1961–1990) and PCM1-A2 future period (2070–2099). The vegetation class mapped at each grid cell is the most frequent class simulated during the time period
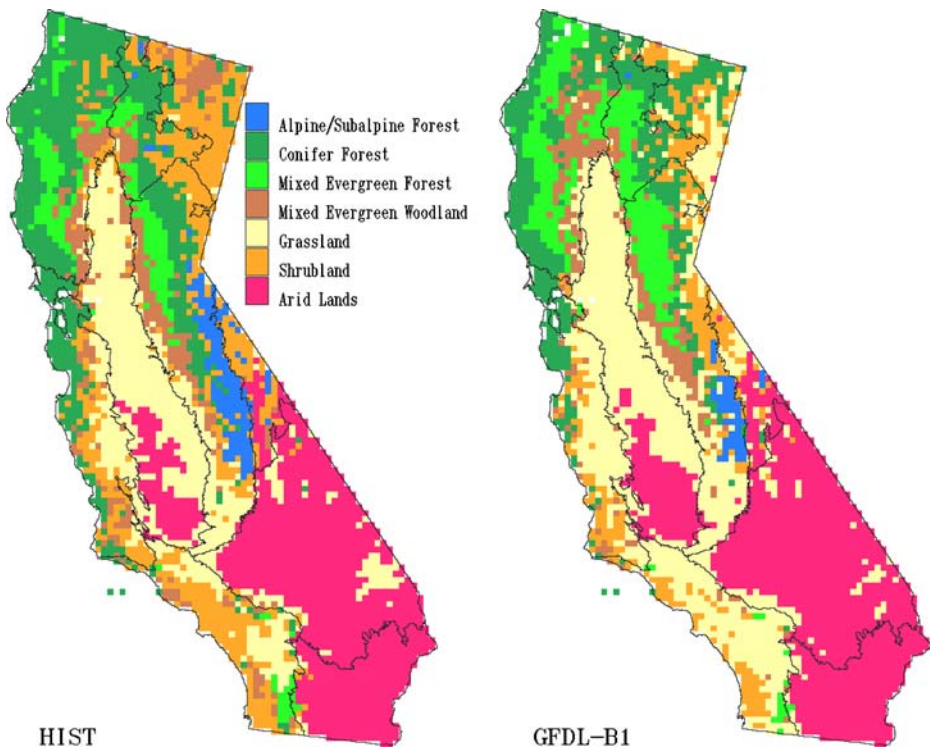
Fig. 2 Distribution of the vegetation classes simulated for the historical (1961–1990) and GFDL-B1 future period (2070–2099). The vegetation class mapped at each grid cell is the most frequent class simulated during the time period

Evergreen Conifer Forest declined under all scenarios, but the largest declines were simulated under the warmer and drier GFDL scenarios. Much of the simulated loss of this type was due to replacement by Mixed Evergreen Forest with increases in temperature, but reductions in effective moisture and increases in fire also resulted in losses of Evergreen Conifer Forest to Woodland, Shrubland, and Grassland. The conversion of Evergreen Conifer Forest to Mixed Evergreen Forest under the cooler and less dry PCM-A2 scenario was largely offset by gains in the semi-arid regions of the Modoc Plateau and Central Coast where Evergreen Conifer Forest advanced primarily into Shrubland.

Mixed Evergreen Forest increased in extent under all three scenarios. Increases in temperature reduced the dominance of the evergreen needleleaf life-form, converting Evergreen Conifer Forest to Mixed Evergreen Forest. The expansion of this type was particularly significant under the PCM-A2 scenario, in which higher levels of effective moisture generally promoted the expansion of forest.

The simulated extent of forest cover (i.e., the combined extent of Evergreen Conifer Forest and Mixed Evergreen Forest) increased relative to the historical extent by 23% under the PCM-A2 scenario. Forest cover declined by 3 and 25% under the GFDL-B1 and GFDL-A2 scenarios, respectively.

Mixed Evergreen Woodland and Shrubland declined under all three scenarios. Under the warmer and drier GFDL scenarios, replacement of these two types, primarily by Grassland, was due to reductions in effective moisture and increased fire. Under the cooler and wetter
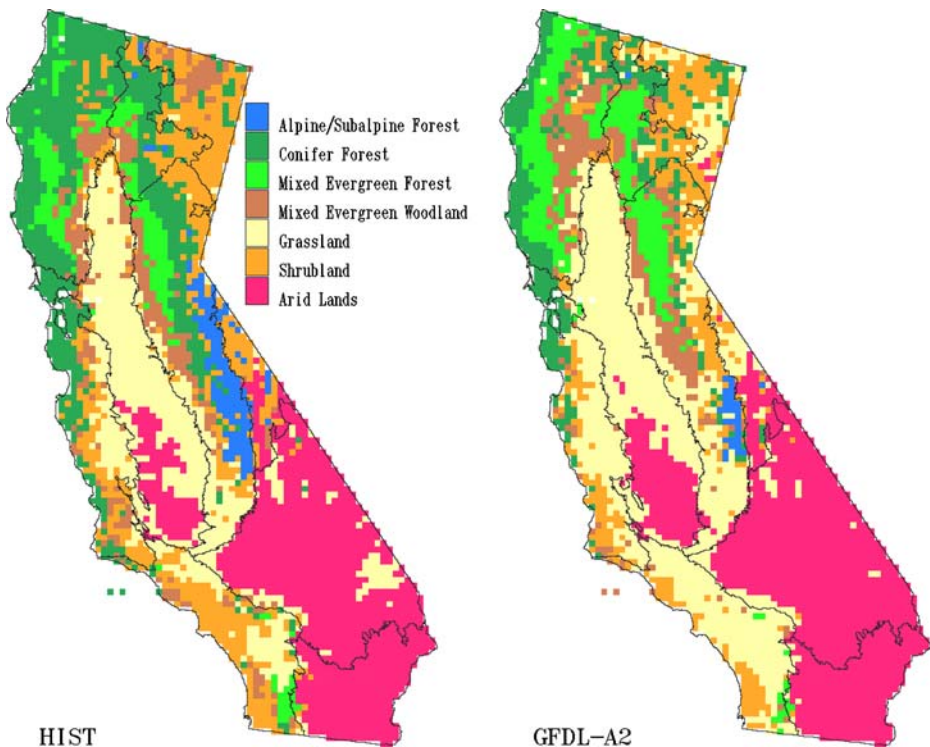
Fig. 3 Distribution of the vegetation classes simulated for the historical (1961–1990) and GFDL-A2 future period (2070–2099). The vegetation class mapped at each grid cell is the most frequent class simulated during the time period

PCM-A2 scenario, the decline in Woodland and Shrubland was not only due to grassland increase, but also to forest encroachment.

Expansion of Grassland under the warmer and drier GFDL scenarios was largely due to reductions in effective moisture. But Grassland gained in extent even under the cooler and less dry PCM-A2 scenario, especially in the semi-arid regions of the state. Here higher levels of effective moisture favored increased productivity of both woody life-forms and grass. However, increases in grass biomass translated to more fine flammable fuels, promoting more fire which in turn reduced the cover of the woody life-forms, resulting in the expansion of grasslands.

The Desert type was reduced in extent by the encroachment of Grassland under the wetter PCM-A2 scenario, but increased at the expense of Grassland under the drier GFDL scenarios.

3.2 The response of ecosystem productivity to the future climate scenarios

Simulated ecosystem net primary productivity (NPP) showed considerable interannual and interdecadal variability, especially over the first half of the twenty-first century when NPP was frequently greater than normal (i.e., greater than the simulated mean annual NPP of 201 teragrams (Tg) per year for the 1895–2003 historical period), even under the drier GFDL scenarios. From about mid-century on, there was a general increasing trend in NPP under
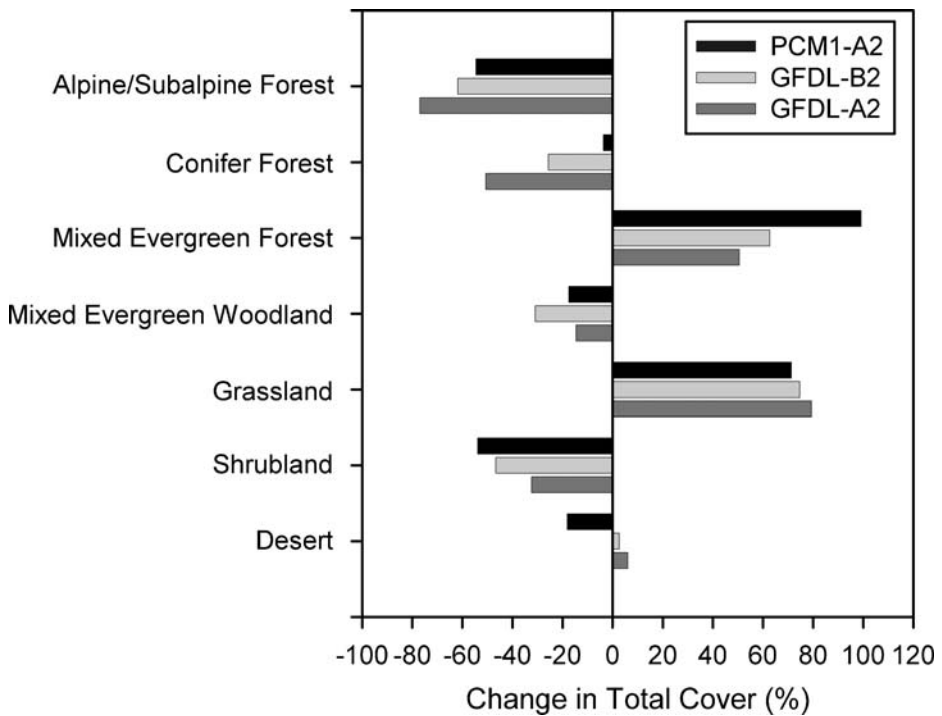
Fig. 4 Percentage change in the total cover of the vegetation classes

the cooler and less dry PCM-A2 scenario, and a general decreasing trend under the warmest and driest GFDL-A2 scenario (Fig. 5a).

A model sensitivity analysis was conducted to assess the contribution of the direct effects of CO_2 (i.e., enhanced plant production and water use efficiency) on the simulated NPP trends. Results indicated that direct CO_2 effects enhanced NPP by about 6% at 500 ppm (concentration at the end of century under the B1 emission scenario) and by about 18% at 800 ppm (concentration at end of century under the A2 emission scenario).

The simulated trend in cumulative net biological production (i.e., NBP, the balance between carbon gained via net primary productivity and carbon lost via decomposition and consumption by fire) showed a steady increase over the course of the future period under the cooler and less dry PCM-A2 scenario (Fig. 5b), resulting in the accumulation of 321 Tg of new ecosystem carbon in California by the end of the century (a 5.5% increase over the total carbon stocks simulated for the historical period, Table 2). New soil/litter carbon accounted for over 80% of the new carbon sink under the PCM-A2 scenario (Fig. 6a). The remaining 20% accumulated as live vegetation carbon, 80% of which was new grass carbon (Fig. 6c).

The simulated trends in cumulative NBP under the warmer and drier GFDL scenarios (Fig. 5b) showed a steady decrease over the course of the future period, resulting in the loss of 76 and 129 Tg (83.8 and 142.2 million tons) of total ecosystem carbon by the end of the century under the B1 and A2 emission scenarios, respectively (Table 2). These losses represent a decline in total carbon stocks of 1.3% (B1) and 2.2% (A2) relative to simulated historical levels. Losses of live vegetation carbon accounted for 80% (B1) and 67% (A2) of the declines in total ecosystem carbon. Losses in total vegetation carbon under the GFDL
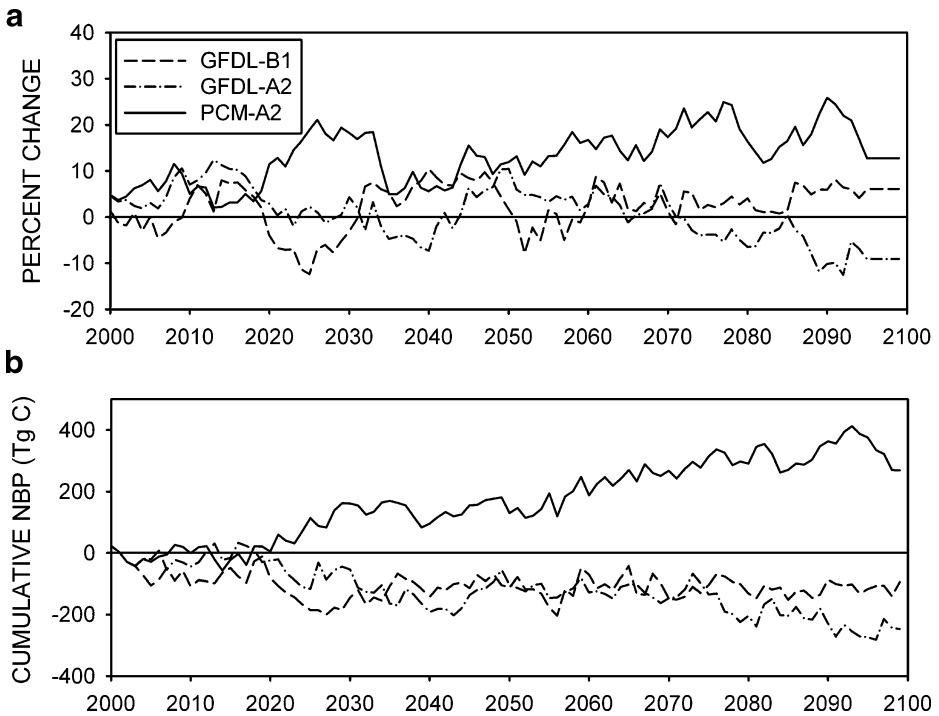
Fig. 5 **a** Percent change in annual net primary production (*NPP*) relative to simulated mean annual NPP for the 1895–2003 historical period, and **b** cumulative net biological production over the future period. NPP trends have been smoothed using a 10-year running average

scenarios were a net result of woody carbon losses and grass carbon gains (Fig. 6b,c). Relative to simulated historical levels, total woody carbon declined by 29% while total grass carbon increased by 22% by the end of the century under the B1 emission scenario. Under the A2 scenario, woody carbon declined by 36% while grass carbon increased by 20%.

3.3 The response of fire to the future climate scenarios

The future trends in simulated total area burned in California were characterized by considerable interannual variability (Fig. 7a), but for nearly every year during the future period, total area burned was greater than the simulated mean total annual area burned over

Table 2 Size of the historical and future carbon pools simulated for the state of California, USA

Carbon pool	Historical	GFDL-B1	GFDL-A2	PCM-A2
Total ecosystem	5,841	5,765	5,712	6,162
Soil and litter	5,359	5,344	5,316	5,624
Total live Vegetation	482	421	396	538
Live wood	330	235	213	340
Live grass	152	186	183	198

All values are in teragrams of carbon. Historical values are the mean masses simulated for the 1895–2003 period. Values for the future climate scenarios are mean masses simulated for the 2070–2099 period.
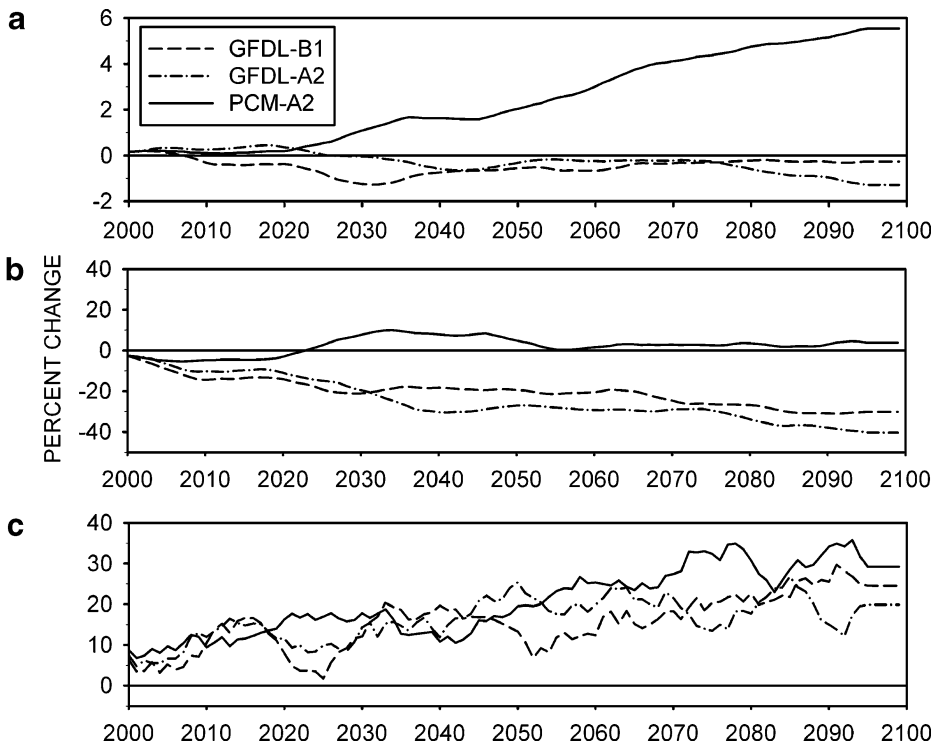
Fig. 6 Percent change in **a** total soil and litter carbon, **b** total live woody carbon, and **c** total live grass carbon relative to simulated mean annual values for the 1895–2003 historical period. All trend lines have been smoothed using a 10-year running average

the 1895–2003 historical period. By the end of the century, predicted total annual area burned ranged from 9% to 15% greater than historical. The greater extent of grasslands (Figs. 1, 2 and 3) and increasing trends in total grass carbon (Fig. 6c) promoted greater rates of simulated fire spread and thus more area burned under all three scenarios.

Predicted future trends in annual total biomass burned (Fig. 7b) were linked to the simulated trends in NPP (Fig. 5a). Under the cooler and less dry PCM-A2 scenario, higher than normal NPP throughout much of the scenario period produced more fuel biomass for consumption. Biomass consumption was about 18% greater than the historical norm by the end of the century under this scenario. Under the warmer and drier GFDL scenarios, simulated biomass consumption was also greater than normal for the first few decades of the century as drought-stressed woodlands and shrublands burned and were converted to grassland. After this transitional period, lower than normal NPP produced less fuel, and biomass consumed was at, or below, the historical norm by the end of the century under the GFDL scenarios.

Spatial variation in the simulated changes in area burned under each scenario (Fig. 8) was largely a product of changes in vegetation productivity and in the competitive balance between woody plants and grasses. Under all three scenarios, the greatest increases in annual area burned were simulated along the central and south coasts, in the northern Great Valley, on the Modoc Plateau, and along the eastern edge of the Sierra Nevada. Here the response of the model to decreased effective moisture under the GFDL scenarios was an increase in the dominance of the more drought-tolerant grasses. And although the response
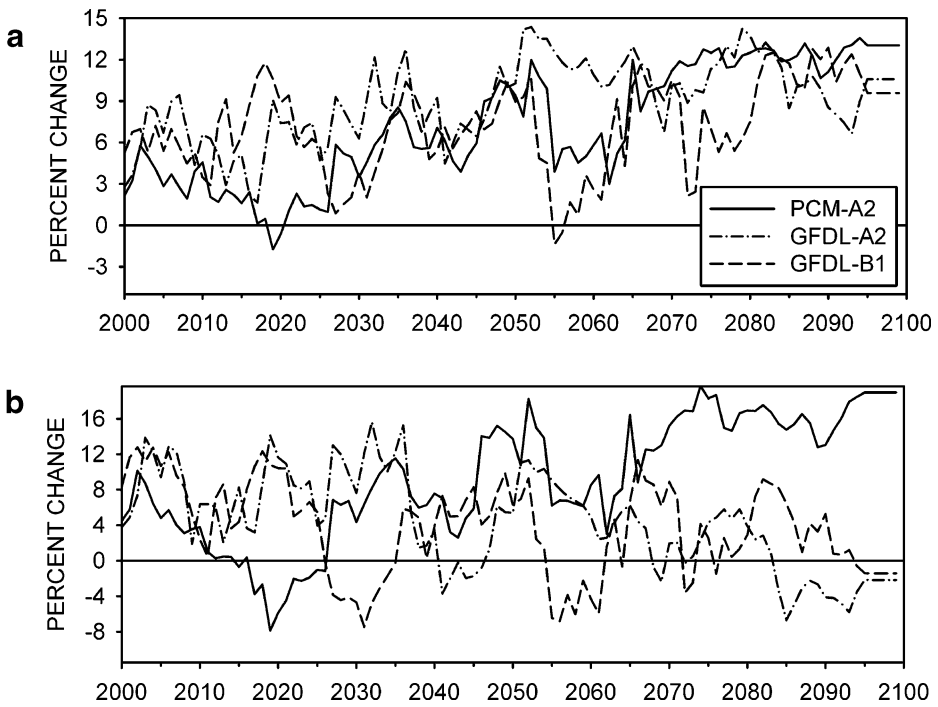
Fig. 7 **a** Percent change in annual total area burned relative to the simulated mean annual total area burned for the 1895–2003 historical period, and **b** percent change in annual total biomass consumed relative to the simulated mean annual biomass consumed for the historical period. All trend lines have been smoothed using a 10-year running average
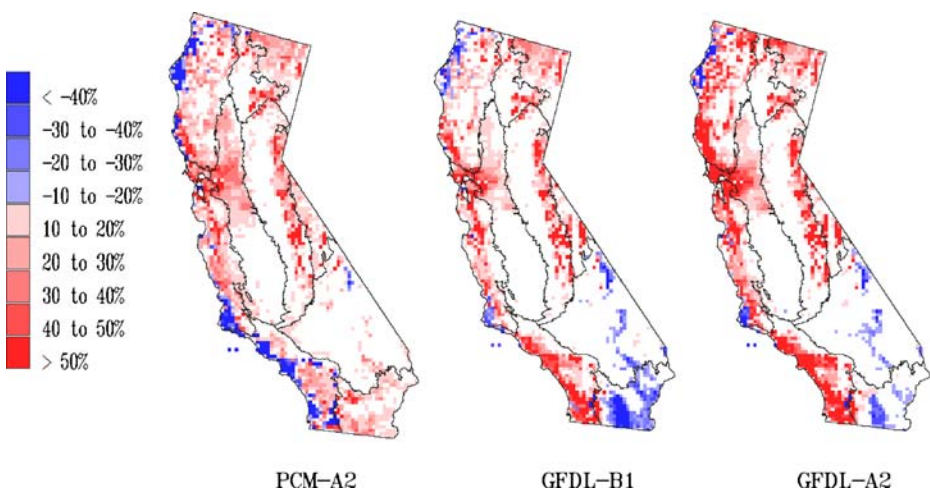

Fig. 8 Percent change in mean annual area burned for the 2050–2099 future period relative to the mean annual area burned for the historical period (1895–2003)

to moderate increases in effective moisture under the PCM-A2 scenario was increased productivity of both life-forms, increases in grass biomass translated to more fine flammable fuels in the model, promoting more fire that in turn reduced the density of the woody life-forms. So under all three scenarios, the response of the model in these semi-arid regions was characterized by a shift towards more grass-dominated vegetation (Figs. 1, 2 and 3) which in turn promoted higher rates of fire spread, and thus more annual area burned.

4 Discussion

The results of the three new MC1 simulations for California generally reinforce those generated under other future climate scenarios (Lenihan et al. 2003; Hayhoe et al. 2004), and demonstrate certain ecosystem sensitivities and interactions that are likely to be features of the response of both natural and semi-natural (e.g., managed forests and rangelands) systems to a relatively certain rise in temperature and less-certain changes in precipitation. For example, reductions in the areal extent of Alpine/Subalpine Forest with increases in growing season warmth were simulated under nine different climate scenarios, with losses averaging 66% across all scenarios. Losses of this vegetation type under GFDL-A2 climate scenario in this study, the second warmest scenario of the nine examined, were especially large (−77%). Extensive conversion of Conifer Forest to Mixed Evergreen Forest with increases in minimum temperatures was also simulated under all nine scenarios, with an average loss of 20%. Reductions in the extent of this commercially important forest type were also especially large (−51%) under the GFDL-A2 scenario in this study.

The model results indicate fire will play a critical role in the adjustment of semi-arid vegetation to altered precipitation regimes, be it slowing or limiting the encroachment of woody vegetation into grasslands under less dry conditions, or hastening the transition from woody communities to grassland under drier conditions. Field observations from coastal central California show that these woody communities have weak resilience to frequent fire and are readily replaced by grassland with higher fire frequency (Keeley 2002; Callaway and Davis 1993). The net losses and redistribution of woodland and shrubland and gains in grassland simulated under the three scenarios in this study are also consistent with the results of MC1 simulations for six other climate scenarios (Lenihan et al. 2003; Hayhoe et al. 2004). Across all nine scenarios, losses of woodland and shrubland averaged 29 and 48% respectively, while gains in grassland averaged 68%. Future reductions in the extent of woodland were also predicted by a statistical climate envelope model developed for California oak woodlands and higher-resolution climate scenarios (Kueppers et al. 2005).

The model results from this study and other MC1 simulations for California also suggest that changes in fire and shifts in the relative dominance of woody and grass life-forms could buffer the effect of different climatic perturbations on total ecosystem carbon storage. For example, even under the wettest scenario examined for California, in which statewide annual precipitation was projected to increase by nearly 75%, MC1 simulated an increase in annual area burned of about 8% in the last few decades of this century (Lenihan et al. 2003). Despite significant increases in net primary production under this warmer and much wetter scenario, increased biomass consumption with increased fire limited increases in carbon storage to about 5% of historical levels. MC1 simulations for drier climate scenarios indicate that decreased carbon storage with the decreased vegetation productivity could be limited by decreased rates of decomposition and a shift towards greater dominance of grass life-forms which are better adapted to more frequent fire and are more effective contributors

to soil carbon stocks. For example, simulation results for this study's GDFL A2 scenario, in which statewide annual precipitation declines by about 22%, show both a decline in vegetation productivity and increase in annual area burned. However, consequent losses to the total ecosystem carbon pool (2% by the end of the century) were limited by a 20% increase in grass carbon which is largely protected from fire belowground and renewed annually aboveground.

Considerable uncertainty exists with respect to the regional-scale impacts of global warming. Much of this uncertainty resides in the differences among different GCM climate scenarios and assumed trajectories of future greenhouse gas emissions, as illustrated in this study. In addition, ecosystem models and their response to projected climate change can always be improved through testing and enhancement of model processes. Dynamic general vegetation models are an especially new technology still undergoing rapid development to improve existing algorithms and introduce new ones. Currently, DGVMs simulate only natural (i.e., unmanaged) vegetation and fail to account for pests and pathogens, non-native invasive plant species, spatio-temporal variation in fire ignition sources, activities such as logging, grazing, agriculture, and urbanization, and other potentially important factors. It is unclear how climate change will impact these factors and their interaction with natural ecosystems, but in some cases, the effects could result in vegetation responses not predicted by extant DGVMs.

The direct effect of increasing atmospheric CO_2 concentration on vegetation productivity and water-use efficiency is another source of uncertainty in DGVM formulation. Free-air CO2 enrichment (FACE) experiments in young forest stands have shown a 23% increase in forest NPP for CO_2 concentrations of 550 ppm as compared to ambient concentrations (Norby et al. 2005). However, Caspersen et al. (2000) showed no evidence of growth enhancement from increased CO_2 in various mature forests of the eastern USA from 1930 to 1980. Recent FACE results from a mature western European deciduous forest also showed no growth enhancement (Körner et al. 2005). Moreover, the CO_2 effect is constrained by water and nutrient availability, even in young stands (Oren et al. 2001; Norby et al. 2005). The CO_2 effect on tree productivity simulated by MC1 (~8% increase in NPP at 550 ppm) is low compared to FACE results from young forest stands. However, MC1 simulates the growth of young to mature stands subject to the constraints of water availability, so CO_2 enhancement of tree growth may not be greatly underestimated in the model. The CO_2 effect on grass productivity simulated by MC1 is the same as for tree productivity (i.e., ~8% increase in NPP at 550 ppm). Herbaceous systems showed an average 14% increase in aboveground biomass with a doubling of CO_2 across nine field experiments, but results varied widely and included declines in production for some systems and increases of up to 85% in others (Mooney et al. 1999. A multi-factor experiment in a California grassland showed no significant response to increased CO_2 (Dukes et al. 2005).

The uncertainty due to differences among future climate scenarios and to unrepresented or poorly understood processes preclude the use of these simulations as unfailing predictions of the future. Nevertheless, the results of this and previous studies underscore the potentially large impacts of climate change on California ecosystems, and the need for further analyses of both future climate change and terrestrial ecosystem responses.

References

Aber J, Neilson R, McNulty S, Lenihan J, Bachelet D, Drapek R (2001) Forest processes and global environmental change: predicting the effects of individual and multiple stressors. Bioscience 51(9):735–751

Anderson GK, Ottmar RD, Prichard SJ (2005) CONSUME 3.0 User's Guide. Pacific Wildland Fire Sciences Laboratory, USDA Foreset Service Pacific Northwest Research Station. Seattle, WA, 183 p

Bachelet D, Lenihan J, Daly C, Neilson R (2000) Interactions between fire, grazing and climate change at Wind Cave National Park, SD. Ecol Model 134:229–224

Bachelet D, Neilson RP, Lenihan JM, Drapek RJ (2001) Climate change effects on vegetation distribution and carbon budget in the U.S. Ecosystems 4:164–185

Barbour M, Pavlik B, Drysdale F, Lindstrom S (1993) California's changing landscapes: diversity and conservation of California vegetation. California Native Plant Society, 246 pp

Callaway RM, Davis F (1993) Vegetation dynamics, fire, and the physical environment in coastal central California. Ecology 74:1567–1578

Caspersen JP, Pacala SW, Jenkins JC, Hurtt GC, Moorcroft PR, Birdsey RA (2000) Contributions of land-use history to carbon accumulation in U.S. forests. Science 290:1148–1151

Cayan D, Luers AL, Hanemann M, Franco G (2006) Scenarios of climate change in California: an overview. Report from the California Climate Change Center. Sacramento, CA. CEC-500-2005-186-SF, 47 p

Cohen JD, Deeming JE (1985) The National Fire Danger Rating System: basic equations. USDA Forest Service Pacific Southwest Forest and Range Experimental Station General Technical Report PSW-82, 16 p

Daly C, Neilson RP, Phillips DL (1994) A statistical-topographic model for mapping climatological precipitation over mountainous terrain. J Appl Meteorol 33:140–158

Daly C, Bachelet D, Lenihan J, Parton W, Neilson R, Ojima D (2000) Dynamic simulations of tree-grass interactions for global change studies. Ecol Appl 10:449–469

Davis FW, Stoms DM, Hollander AD, Thomas KA, Stine PA, Odion D, Borchert MI, Thorne JH, Gray MV, Walker RE, Warner K, Graae J (1998) The California Gap Analysis Project, Final Report. University of California, Santa Barbara, CA

Dukes J, Chiariello N, Cleland E, Moore L, Shaw M, Thayer S, Tobeck T, Mooney H, Field C (2005) Response of grassland production to single and multiple global environmental change. PLoS Biology 3(10):319e

Hayhoe K, Cayan D, Field C, Frumhoff P, Maurer E, Miller N, Moser S, Schneider S, Cahill K, Cleland E, Dale L, Drapek R, Hanemann R, Kalkstein L, Lenihan J, Lunch C, Neilson R, Sheridan S, Verville J (2004) Emission pathways, climate change, and impacts on California. Proc Natl Acad Sci U S A 101:12422–12427

Holland V, Keil D (1995) California vegetation. Kendall/Hunt, Dubuque, Iowa 515 p

Intergovernmental Panel on Climate Change (2000) Special Report on Emissions Scenarios. In: Nakicenovic N, Swart R (eds) Cambridge University Press, UK, 570 pp

Kattenberg A, Giorgi F, Grassl H, Meehl G, Mitchell J, Stouffer R, Tokioka T, Weaver A, Wigley T (1996) Climate models: projections of future climate. In: Houghton JL, Filho M, Callander B, Harris N, Kattenberg A, Maskell K (eds) Climate change 1995: the science of climate change. Contribution to Working Group 1 to the Second Assessment Report of the Intergovernmental Panel on Climate Change. Cambridge University Press, Cambridge, UK, pp 285–357

Keeley JE (2002) Native American impacts on fire regimes of the California coastal ranges. J Biogeogr 29:303–320

Kittel TGF, Rosenbloom NA, Royle JA, Daly C, Gibson WP, Fisher HH, Thornton P, Yates DN, Aulenbach S, Kaufman C, McKeown R, Bachelet D, Schimel DS, VEMAP2 Participants (2004) VEMAP phase 2 bioclimatic database. I. Gridded historical (20th century) climate for modeling ecosystem dynamics across the conterminous United States. Clim Res 27:151–170

Körner C, Asshoff R, Bignucolo O, Hättenschwiler S, Keel SG, Peláez-Riedl S, Pepin S, Siegwolf RTW, Zotz G (2005) Carbon flux and growth in mature deciduous forest trees exposed to elevated CO_2. Science 309:1360–1362

Kueppers LM, Snyder MA, Sloan L, Zavaleta ES, Fulfrost B (2005) Modeled regional climate change and California endemic oak ranges. Proc Nat Acad 102(45):16281–16286

Lenihan JM, Drapek R, Bachelet D, Neilson R (2003) Climate change effects on vegetation distribution, carbon, and fire in California. Ecol Appl 13(6):1667–1681

Mooney H, Canadell J, Chapin F, Ehleringer J, Korner C (1999) Ecosystem physiology responses to global change. In: Walker B, Steffen W, Canadell J, Ingram J (eds) The terrestrial biosphere and global change. Cambridge University Press, Cambridge, U.K., pp 141–189

Norby RJ, Luo Y (2004) Evaluating ecosystem responses to rising atmospheric CO_2 and global warming in a multi-factor world. New Phytologist 162:281–293

Norby RJ, DeLucia EH, Gielen B, Calfapietra C, Giardina CP, King JS, Ledford J, McCarthy HR, Moore DJP, Ceulemans R, De Angelis P, Finzi AC, Karnosky DF, Kubiske ME, Lukac M, Pregitzer KS, Scarascia-Mugnozza GE, Schlesinger WH, Oren R (2005) Forest response to elevated CO_2 is conserved across a broad range of productivity. Proc Natl Acad Sci U S A 102:18052–18056

Oren R, Ellsworth DS, Johnsen KH, Phillips N, Ewers BE, Maier C, Schafer KVR, McCarthy H, Hendrey G, McNulty SG, Katul GG (2001) Soil fertility limits carbon sequestration by forest ecosystems in a CO2 enriched world. Nature 411:469–472

Parton W, Schimel D, Ojima D, Cole C (1994) A general study model for soil organic model dynamics, sensitivity to litter chemistry, texture, and management. SSSA Special Publication 39. Soil Sci Soc Am 147–167

Peterson D, Ryan K (1986) Modeling postfire conifer mortality for long-range planning. Environ Manage 10:797–808

Rothermel R (1972) A mathematical model for fire spread predictions in wildland fuels. USDA Forest Service Research Paper INT-115, 40 pp

Strauss D, Bednar L, Mees R (1989) Do one percent of forest fires cause ninety-nine percent of the damage? For Sci 35:319–328

Turner M, Romme W (1994) Landscape dynamics in crown fire ecosystems. Landsc Ecol 9(1):59–77

van Wagner CE (1993) Prediction of crown fire behavior in two stands of jack pine. Can J For Res 23:442–449